KSCE Journal of Civil Engineering (2016) 20(1):175-187
DOI 10.1007/s12205-015-0464-3

Environmental Engineering
pISSN 1226-7988, eISSN 1976-3808
www.springer.com/12205

Kinetics of Nitrate Adsorption and Reduction by Nano-scale Zero Valent Iron (NZVI): Effect of Ionic Strength and Initial pH

Do-Gun Kim*, Yu-Hoon Hwang, Hang-Sik Shin***, and Seok-Oh Ko******

Received August 18, 2014/Revised February 15, 2015/Accepted February 24, 2015/Published Online April 3, 2015

Abstract

Kinetic models for pollutants reduction by Nano-scale Zero Valent Iron (NZVI) were tested in this study to gain a better understanding and description of the reaction. Adsorption kinetic models and a heterogeneous catalytic reaction kinetic equation were proposed for nitrate removal and for ammonia generation, respectively. A widely used pseudo-first-order reaction model was a poor fit for nitrate removal in an iron-limiting condition and for ammonia generation in an excess iron condition. However, in this study, pseudo-first-order and pseudo-second-order adsorption kinetic equations were a good fit for nitrate removal; in addition, a Langmuir-Hinshelwood kinetic equation was able to successfully describe ammonia generation, regardless of the NZVI dose, the ionic strength, and the initial pH. These results strongly indicate that nitrate reduction by NZVI is a heterogeneous catalytic reaction, and that that the kinetic models can be used in diverse conditions. The kinetic parameters correlate well with the reaction condition, unless the NZVI dose was greatly increased or unless the NZVI surface was significantly changed at a very high initial pH.

Keywords: *adsorption, heterogeneous catalytic reaction, ionic strength, kinetics, NZVI, pH*

1. Introduction

Chemical reduction of water pollutants, such as nitrate, chlorinated organic compounds, and heavy metals, by Nano-scale Zero Valent Iron (NZVI), has gained attention (Hwang *et al*., 2012; Lin *et al*., 2008b; Liu *et al*., 2012; Petala *et al*., 2013). However, a proper reaction kinetic model has not been proposed. Until recently, pseudo-homogeneous reaction kinetics has been used to describe the NZVI-induced reduction of nitrate and other pollutants. Satapanajaru *et al*. (2011) described Reactive Black 5 and Reactive Red 198 removal by NZVI with a specific surface area normalized pseudo-first-order-reaction kinetics equation. Petala *et al*. (2013) and Zhang *et al*. (2009) used pseudo-first-order reaction kinetics equation to describe Cr(VI) removal by MCM-41 immobilized NZVI and 2,4,6-Trinitrotoluene reduction by NZVI, respectively. However, pseudo-first-order reaction kinetics offers a poor description, especially in iron-limiting conditions; that is, where the iron dose is insufficient to remove all the pollutant in a system (Liu *et al*., 2005; Andreas *et al*., 2009; Alidokht *et al*., 2011; Satapanajaru *et al*., 2011), although the pseudo-first-order reaction kinetic model is the most widely used and it describes well the pollutants reduction by microscale iron powders (Andreas *et al*., 2009). Therefore, no kinetics analysis was given in some studies using NZVI. Liu *et al*. (2012) investigated the nitrate reduction according to reaction time by NZVI prepared by hydrogen reduction of goethite, but they did not provide kinetic analysis. In addition, Huang *et al*. (1998) and Yang and Lee (2005) observed that the reaction order varied in relation to the NZVI dose and the initial nitrate concentration.

Furthermore, heterogeneous catalytic reaction models have not been proposed for NZVI, even though NZVI can be regarded as a heterogeneous catalyst. In addition, the kinetics of product generation from a chemical reduction by NZVI have seldom been investigated. Recently, Zhang *et al*. (2013) investigated nitrobenzene reduction and byproduct (aniline) generation by NZVI immobilized in channels of ordered mesoporous silica. However, they did not propose kinetic models neither for the nitrobenzene removal nor for the aniline generation. For nitrate reduction by NZVI, Ammonia is generally known as a major product (Liu *et al*., 2005; Hwang *et al*., 2010). The amount of ammonia generated is less than the stoichiometric amount of nitrate removed when NZVI is used. In addition, in many studies with NZVI, the total amount of nitrogen initially decreases and then increases (Huan *et al*., 2006; Wang *et al*., 2006; Lin *et al*., 2008b). It has been regarded that the decrease of the total nitrogen is due to the generation of gaseous nitrogen species

*Research Professor, Dept. of Civil Engineering, Kyung Hee University, Yongin 446-701, Korea (E-mail: dogun.kim@khu.ac.kr)
**Researcher, Dept. of Environmental Engineering, Technical University of Denmark, Lyngby 2800, Denmark (E-mail: yuoh@env.dtu.dk)
***Member, Professor, Dept. of Civil and Environmental Engineering, Korea Advanced Institute of Science and Technology, Daejeon 305-338, Korea (E-mail: hangshin@kaist.ac.kr)
****Member, Professor, Dept. of Civil Engineering, Kyung Hee University, Yongin 446-701, Korea (Corresponding Author, E-mail: soko@khu.ac.kr)

(Liou *et al*., 2005; Yang and Lee, 2005; Huan *et al*., 2006; Wang *et al*., 2006). However, this explanation does not fully account for the decrease and subsequent increase of the total nitrogen during the reaction with NZVI. In addition, the nitrate reduction to gaseous nitrogen, i.e., N_2, is not thermodynamically favorable (Choe *et al*., 2000; Alowitz *et al*., 2002). The ammonia generation rate is therefore slower than the nitrate removal (Li *et al.*, 2008) and the adsorbed and unreacted nitrate on the NZVI surface undergoes a further surface reaction to the ammonia or nitrite that is to be desorbed in the aqueous phase. The retardation of ammonia generation is not generally observed for microscale Zero Valent Iron (ZVI) or other catalysts which have a lower nitrate reduction rate than NZVI, therefore, the nitrogen mass balance was almost complete during whole reaction time when they were used (Huang *et al*., 2003; Huang and Zhang, 2004; Su and Puls, 2004; Luo *et al*., 2014).

In this study, the nitrate removal and ammonia generation were described separately, based on the findings cited above. Adsorption kinetic modes were proposed for nitrate removal, while ammonia generation was described as a heterogeneous catalytic reaction. In addition, the effects of the NZVI dose, initial pH, and ionic strength were evaluated with the kinetic models. How ionic strength affects the performance of a water treatment alternative is one of the most important factors. Note, for example, that the retentates from the membrane process have a high ion concentration and a high level of conductivity (García-Figueruelo *et al*., 2009). Most of the relevant literature confirms the dependency on pH but only for acidic conditions because, iron hydroxide precipitates, which have an adverse effect, tend to form at a high pH level (Huang and Zhang, 2004; Wang *et al*., 2006). However, the nitrate reduction at a pH range of 3 to 11 was investigated in this study for a better understanding of the pH effect.

2. Materials and Methods

2.1 Preparation of NZVI

In this study, NZVI was prepared in an aqueous solution of Deoxygenated Deionized Water (DDIW) via the reduction of ferric ion (Fe^{3+}) with sodium borohydride (Wang and Zhang, 1997). A 200 mL sodium borohydride solution (223.834 mM, Kanto) was introduced dropwise at a flow rate of 5 mL/min to a 150 mL ferric ion solution (59.689 mM, Kanto) in a 1 L round flask. The NZVI slurry was aged for 20 min and filtered with a 0.45 μm cellulose-acetate membrane filter to collect NZVI particles. The NZVI was separated easily by filtration because NZVI particles aggregate in an aqueous solution without a stabilizing agent (Yang and Lee, 2005). The NZVI was washed and centrifuged several times with a large volume of DDIW before being injected into the reactor. A laser scattering device (ZetaPlus, Brookhaven Instruments Corporation) showed that the average particle diameter of NZVI was 16.7 nm and the BET surface area was 17.623±0.042 m^2/g (Sorptomatic 1990, Thermo Electron Corporation).

2.2 Batch Experiment

Batch experiments were conducted in a 1 L Schlenk flask at room temperature (20±2°C) with continuous stirring. A nitrate solution was prepared with DDIW and purged again with N_2 for 2 h before the start of a reaction. The openings of the Schlenk flask were sealed with stoppers, and N_2 gas was bubbled at 0.2 L/min during the reaction to maintain an anoxic condition. The NZVI was put into the reactor, and the mixture was agitated at 250 rpm. Samples were taken periodically and filtered with 0.45 ìm syringe filters for immediate analysis. The initial nitrate concentration was 50 mg-N/L for all experiments. The time course of the nitrate and ammonia concentration was investigated at an NZVI dose of 0.2 to 2.0 g/L to test and evaluated the reaction kinetic models for nitrate reduction. The effects of the ionic strength (0.05-0.5 M NaCl) and initial pH (3-11) were investigated in relation to 0.5 g/L NZVI. The initial pH was adjusted with 0.05, 0.5, and 5 N NaOH and 0.01, 0.1, and 1 N HCl. The nitrate stock solution (1000 mg-N/L) was prepared with KNO_3 (Duksan). All the batch tests were done in duplicate or triplicate, and the average values are presented because the errors are less than 5%. The nitrate and nitrite concentrations were analyzed by means of ion chromatography (DX-120, Dionex), and the ammonia was analyzed in accordance with the 20th edition of Standard Methods (AWWA-APHA-WPCF, 1998).

2.3 Kinetic Models

The stoichiometric relations used in this study involve nitrate, iron metal, and proton as reactants and incorporated ammonium, Fe(II), and water as products (Yang and Lee, 2005). Several assumptions about kinetic equations were derived from the literature and the findings of this study.

The first assumption is that the nitrate reduction by NZVI is a heterogeneous catalytic reaction. It seems that adsorption contributes to the apparent removal of nitrate before the reduction of nitrate to ammonium because the nitrate reduction induced by a heterogeneous catalyst is a surface reaction. Li *et al*. (2008) observed that ammonia generation was slower than nitrate removal when NZVI was used; they subsequently proposed some possible reaction pathways. One reaction pathway was direct reduction to ammonia; another was the reduction that occurs after the nitrate adsorption on NZVI, which results in a decrease of the total nitrogen at the beginning of the reaction. Furthermore, Liou *et al*. (2005) calculated the activation energy of NZVI-induced nitrate reduction to 25.8 kJ/mol which indicates that the dominant mass transport involves, rather than a surface reaction, because the typical mass transfer-controlled reactions in aqueous phase is 10-20 kJ/mol (Spiro, 1989). Note also that nitrate adsorption reportedly occurs on many materials, such as activated carbon and sepiolite (Öztürk and Bektaş, 2004). The above-mentioned results strongly indicate that unreacted nitrate exists on the NZVI surface. The unreacted nitrate was partially recovered by a separate experiment in this study with 0.5 g/L NZVI and 50 mg/L nitrate. Two samples were taken from a reactor: one sample was filtered immediately for analysis;

the other was diluted in Deionized Water (DIW) and purged with air for 1 h to provide an oxic condition for nitrate desorption. The results show that the nitrate concentration of the air-purged samples was higher for the whole reaction period (3 h) than that of the samples, which were immediately analyzed. After 15 min of reaction, the T-N dropped to its minimum value of 40.727 mg-N/L but recovered to 49.834 mg/L after the 1 h desorption of nitrate. The above mentioned findings from the literature and this study strongly indicate that nitrate reduction by NZVI is a heterogeneous catalytic reaction, which can be expressed as follows, assuming hydroxylation of NZVI surface:

$$\equiv S + H^+ \rightarrow \equiv S - H^+ \tag{1a}$$

$$\equiv S - OH + NO_3^- \rightarrow \equiv S - NO_3^- + OH^- \tag{1b}$$

$$S - H^+ + S - NO_3^- \rightarrow NH_4^+ + 3H_2O + 4Fe^{2+} + S \tag{1c}$$

where, S is the surface of NZVI. The reaction in Eq. (1c) is slower than the reaction in Eq. (1b). Therefore, nitrate adsorption and ammonia generation were described separately. The second assumption is that nitrate removal follows adsorption kinetics rather than a pseudo-homogeneous reaction based on the first assumption. The third assumption is that ammonium is the only reaction product. The nitrite concentration was ignored because it was very low. The fourth assumption is that the adsorption/desorption of ammonium was ignored in the results of an earlier study that showed no ammonium adsorption on NZVI (Hwang *et al*., 2010). In the fitting procedure, the constants in the kinetic equations were estimated with a nonlinear regression, minimizing the sum of squares due to error (*SSE*), using MATLAB (MathWorks, USA).

2.3.1 Kinetics of Nitrate Removal

Several models, including the pseudo-first-order reaction model, were tested in this study; the way they describe the behavior of nitrate is expressed below in Eqs. (2) to (7). The study also applies the pseudo-first-order adsorption, the pseudo-second-order adsorption, the Elovich equation, and the intraparticle diffusion model (Câmara and Neto, 2008; Hameed *et al*., 2008; Cáceres-Jensen *et al*., 2013). The following equations were transformed so that they expressed in terms of the nitrate concentration instead of the amount of adsorption:

$$\frac{dC_n}{dt} = -k_{k1} C_n \tag{2}$$

$$\frac{dC_n}{dt} = -k_m C_n^n \tag{3}$$

$$\frac{dq_n}{dt} = k_{a1}(q_{n,e} - q_n), \ \frac{dC_n}{dt} = -k_{a1}(C_n - C_{n,e}) \tag{4}$$

$$\frac{dq_n}{dt} = k_{a2}(q_{n,e} - q_n)^2, \ \frac{dC_n}{dt} = -\frac{k_{a2}}{C_C}(C_n - C_{n,e})^2 \tag{5}$$

$$\frac{dq_n}{dt} = \alpha \cdot \exp(-\beta \cdot q_n), \ \frac{dC_n}{dt} = -\alpha \cdot \exp\left(-\beta \frac{C_{n,0} - C_n}{C_C}\right) \tag{6}$$

$$R = k_{id} \cdot t^{\gamma}, \ \ln\left(\frac{C_{n,0} - C_n}{C_{n,0}}\right) = \ln(k_{id}) + \gamma \ln(t) \tag{7}$$

where, C_n (mg-N/L) is the nitrate concentration at time t (min), k_{r1} (min^{-1}) is the pseudo-first-order reaction rate constant, k_{rn} is the reaction rate constant with the estimated reaction order n, $\underline{q_n}$ (mg-N/g-NZVI) is the adsorbed nitrate amount at time t, $q_{n,e}$ (mg-N/g-NZVI) is the equilibrium adsorption amount of nitrate, k_{a1} (min^{-1}) is the pseudo-first-order adsorption rate constant, k_{a2} (g-NZVI/mg-N·min) is the pseudo-second-order adsorption rate constant, and C_c is the NZCI amount (g-NZVI/L). In the Elovich equation, α (mg-N/g-NZVI·min) is the constant for the initial sorption rate and β (g-NZVI/mg-N) is the constant for the parameter related to the extent of surface coverage and the activation energy of the chemisorption. In the intraparticle diffusion model, k_{id} (min^{-1}) is the constant for the intraparticle diffusion rate and γ is the constant for the adsorption mechanism.

2.3.2 Kinetics of Ammonia Generation

The important phenomenon of ammonia generation has not been considered as a product of catalytic nitrate reduction. For this study, the first estimation of the ammonia concentration is based on a subtraction of the nitrate concentration at each reaction time from the initial nitrate concentration. The ammonia concentration estimation was accurate when microscale ZVI was used (Huang and Zhang, 2003; Huang and Zhang, 2004; Su and Puls, 2004). Then the pseudo-first-order reaction kinetics and a Langmuir-Hinshelwood-type kinetic formulation (Eq. (8)) were tested. The Langmuir-Hinshelwood-type kinetic formulation is based on the following assumptions: the nitrate and proton are adsorbed on the same active site; the nitrate and hydrogen are adsorbed in equilibrium; the reaction is irreversible; the desorption is fast; and no reaction products are adsorbed. In a simplification of the equation, the proton concentration and the equilibrium proton adsorption constant are ignored because they are known to be very small (Pintar *et al*., 1996), It is supported by the pH for all experiments in this study: the pH increased rapidly at the beginning to a range of 10 to 10.5 and then remained steady until the end of reaction. Eq. (8) is expressed as follows:

$$\frac{dC_a}{dt} = \frac{kKC_n}{(1 + KC_n)^2} \tag{8}$$

where, C_a (mg-N/L) is the ammonia concentration, C_n (mg-N/L) is the nitrate concentration, k (mg/L·min) is the reaction rate constant, and K (L/mg) is the equilibrium adsorption constant. In addition, the ammonia concentration was observed to increase and then decrease at a range of 1.0-2.0 g/L NZVI because the ammonia stripping occurred by the inert gas flow, which was applied to prevents NZVI oxidation (Hwang *et al*., 2010). Therefore, ammonia stripping was considered for a better description of ammonia profiles. Quan *et al*. (2009) proposed a kinetic equation of liquid ammonia volatilization, and Patoczka and Wilson (1984) developed an equation for the liquid-gas mass transfer of ammonia. These two equations are expressed respectively as follows:

$$\ln\left(\frac{C_{a,l}}{C_{a,l,0}}\right) = -\frac{Q_g K_H^{'}}{V_l}\left[1-\exp\left(\frac{K_l A V_l}{Q_g K_H^{'}}\right)\right]t = -K_l A t \quad (9)$$

$$\ln\left(\frac{C_{a,l}}{C_{a,l,0}}\right) = -\frac{\alpha Q_g K_H^{'}}{V_l}\left[\frac{k_{a,l,A}}{Q_g}(1-f)+\{1-\exp(-k_{a,g,A}\tau)\}\right] = \frac{\alpha Q_g K_H^{'}}{V_l}t \quad (10)$$

where, $C_{a,l,0}$ (mg/L) and $C_{a,l}$ (mg/L) are the initial and liquid phase ammonia concentration at time t (min), Q_g (L/min) is the gas flow rate, K_H' is the dimensionless Henry's law constant, V_l (L) is the liquid volume, K_l (m/min) is the overall liquid mass transfer coefficient, A (m^2/m^3) is the interface area per unit volume of liquid, α' is the fraction of ammonia (NH_3) in the solution, $k_{a,l,A}$ is the mass transfer coefficient of the free water surface multiplied by the water surface area, $k_{a,g,A}$ is the mass transfer coefficient based on the gas phase, f is the degree of saturation of air entering the space above the liquid surface, and τ is the retention time. Eqs. (9) and (10) can both be simplified to a pseudo-first-order kinetic equation when no ammonia is present in the inlet gas. In view of the ammonia stripping, Eq. (8) can therefore be modified as follows:

$$\frac{dC_a}{dt} = \frac{kKC_n}{(1+KC_n)^2} - k_S C_a \quad (11)$$

where, k_s is the ammonia removal rate constant (min^{-1}). The value of k_s was found to be $6.2 \pm 0.04 \times 10^{-6}$ min^{-1} in separate batch experiments with a solution of 12.5, 25, and 50 mg-NH_4^+-N/L prepared with NH_4Cl (Sigma-Aldrich) at an N_2 gas flow rate of 0.2 L/min. Quan *et al*. (2009) reported that the initial ammonia concentration had a negligible effect on ammonia stripping rate. Therefore the value of k_s was used in this study regardless of ammonia concentration.

3. Results and Discussion

3.1 Kinetics of Nitrate Reduction for Different Doses of NZVI

Figure 1 shows the concentration of nitrate, ammonia, and T-N for 0.2-2.0 g/L NZVI. The ammonia generation was retarded in all experiments, and the T-N recovery was faster with a higher dose of NZVI. The most significant decrease of T-N (due to the slower ammonia generation) was observed at the highest NZVI dose (2.0 g/L), indicating a faster rate of nitrate adsorption under a condition of excess iron.

The nitrate concentration described by the pseudo-first-order reaction kinetic model and pseudo-second-order adsorption equation and was illustrated in Fig. 2(a). The correlations between NZVI dose and the parameters of the pseudo-first-order reaction kinetic model and pseudo-second-order adsorption equation are provided in Fig. 2(b), (c). The nitrate concentration described by an *n*th-order model, pseudo-first-order adsorption kinetics, the Elovich equation, and an intraparticle diffusion model for different NZVI doses, was illustrated in Fig. 6, while the correlations

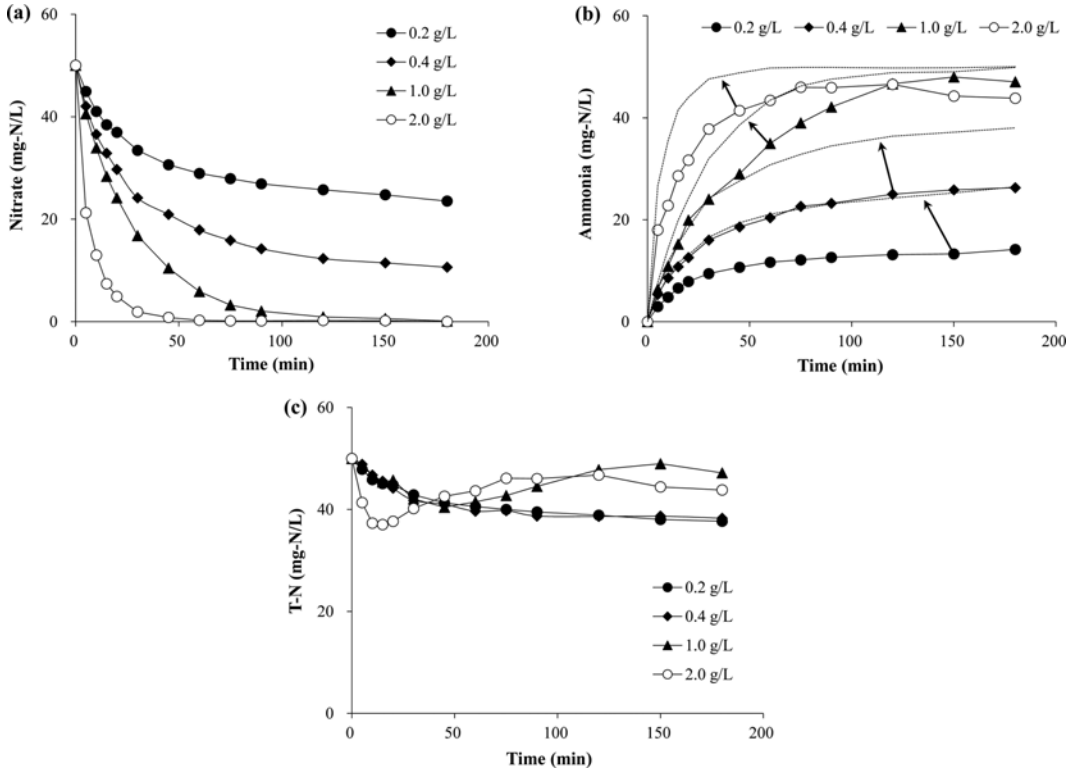

Fig. 1. Profiles of: (a) Nitrate, (b) Ammonia, and (c) T-N During Nitrate Reduction for Different NZVI Doses (C_{NZVI}, The Dotted Lines in, (b) Indicate the Removed Nitrate Nitrogen (NO_3^--N) Concentration at Each NZVI Dose)

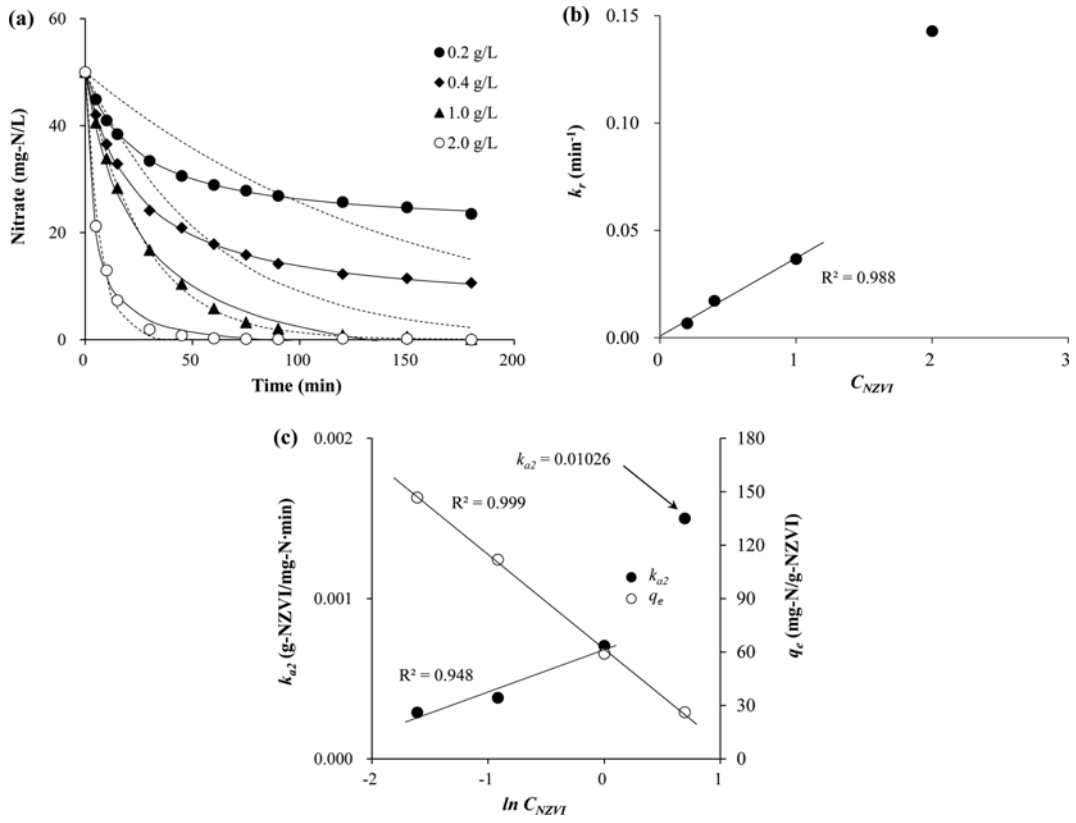

Fig. 2. (a) Predictions of Nitrate Concentration from: (a) Pseudo-first-order Kinetics (Dotted Lines) and Pseudo-second-order Adsorption Kinetics (Continuous Lines) for Different NZVI Doses; the Correlation between the NZVI Dose (C_{NZVI}) and Kinetic Parameters for, (b) the Pseudo-first-order Kinetics and, (c) the Pseudo-second-order Adsorption Kinetics

between the parameters of the kinetic models and NZVI dose are given in Fig. 7. Table 1 lists the parameters obtained by the various kinetic models. The results show that the pseudo-first-order reaction kinetic model is unsuitable for an iron-limiting condition but suitable for an excess iron condition (2.0 g/L NZVI) (Fig. 2(a)). However, the estimated pseudo-first-order rate constant correlates well with the NZVI dose (Fig. 2(b)). For an *n*th order reaction, the reaction rate constant increases and the reaction order decreases as the NZVI dose is increased (Figs. 6(a) and 7(a)). This is consistent with the findings of other studies (Yang and Lee, 2005; Wang *et al*., 2006). Of the tested adsorption kinetic equations, the pseudo-second-order adsorption equation provides the best fit, especially for the iron-limiting condition (Fig. 2(a), (c); Table 1). Good results were also obtained with the pseudo-first-order adsorption kinetic equation but it predicted that a plateau was reached, even though the nitrate adsorption was still in progress at 0.2 to 0.4 g/L NZVI (Fig. 6(b); Table 1). A pseudo-first-order adsorption process can be applied when the mass of adsorbate on a solid surface is low; and pseudo-second-order adsorption kinetics is suitable when the surface concentration of adsorbates is high. A pseudo-second-order adsorption rate equation has been used to demonstrate how the rate depends on the sorption capacity of the solid phase (Ho and Ofomaja, 2006; Cáceres-Jensen *et al*., 2013). That equation is widely used for biosorption and for describing adsorption kinetics under nonequilibrium conditions (Zhou *et al*., 2012). This study therefore investigates how the pH and ionic strength affect pseudo-second-order adsorption kinetics because all the experimental data at various ionic strengths and pH values were obtained with NZVI dose of 0.5 g/L, where the nitrate concentration did not reach a state of equilibrium for all experiments. Furthermore, the nitrate adsorption capacity of NZVI, which was estimated on the basis of pseudo-first-order adsorption or pseudo-second-order adsorption, was higher than the corresponding capacity of other adsorbents such as activated carbon or activated sepiolite (Öztürk and Bektaş, 2004). This result confirms the excellence of NZVI as a nitrate adsorbent. Meanwhile, the intraparticle diffusion model is a poor fit, which implies that intraparticle diffusion does not limit the rate of nitrate sorption on NZVI (Figs. 6(d) and 7(d); Table 1); however, the mass transfer across the external boundary layer of a solid or the boundary-layer diffusion of nitrate is a dominant factor in nitrate adsorption by NZVI (Cheung *et al*., 2007). This is also supported by the good fit of the experimental results to the pseudo-second-order adsorption rate equation (Cáceres-Jensen *et al*., 2013).

Figure 3(a) shows the results of the fit for the ammonia concentration. The prediction of the ammonia concentration is based on the adsorbed nitrate concentration, which was calculated by subtracting the final nitrate concentration from the nitrate concentration at each reaction time. The pseudo-first-order

Table 1. Kinetic Parameters of Nitrate Removal by NZVI for Different NZVI Doses

Kinetic model	NZVI (g/L)	Parameters		*SSE*	r^2
		k_{r1} (min^{-1})			
Pseudo first order reaction	0.2	6.692×10^{-3}		386.114	0.538
	0.4	1.720×10^{-2}		330.066	0.831
	1.0	3.667×10^{-2}		3.113	0.999
	2.0	1.428×10^{-1}		20.020	0.992
		k_{rn}	n		
n^{th} order reaction	0.2	8.059×10^{-9}	4.857	4.000	0.995
	0.4	9.259×10^{-5}	2.560	2.505	0.999
	1.0	2.834×10^{-2}	1.078	1.630	1.000
	2.0	4.108×10^{-2}	1.396	2.557	0.999
		k_{a1} (min^{-1})	q_e (mg-N/g-NZVI)		
Pseudo first order adsorption	0.2	3.767×10^{-2}	123.332	10.309	0.995
	0.4	3.776×10^{-2}	94.180	17.664	0.996
	1.0	3.739×10^{-2}	49.589	2.475	1.000
	2.0	1.485×10^{-1}	24.672	16.601	0.997
		k_{a2} (g-NZVI/mg-N·min)	q_e (mg-N/g-NZVI)		
Pseudo second order adsorption	0.2	2.890×10^{-4}	146.780	0.702	0.999
	0.4	3.815×10^{-4}	111.916	1.133	0.999
	1.0	7.059×10^{-4}	59.077	22.495	0.994
	2.0	1.026×10^{-2}	26.106	11.633	0.995
		α (mg-N/g-NZVI·min)	β (g-NZVI/mg-N)		
Elovich equation	0.2	2.152	2.987×10^{-2}	6.477	0.992
	0.5	3.250	3.898×10^{-2}	20.960	0.989
	1.0	4.073	7.293×10^{-1}	99.627	0.972
	2.0	8.804×10^{2}	3.827×10^{-1}	2430.870	0.957
		k_{id} (min^{-1})	γ		
Intra-particle diffusion	0.2	2.391	3.754×10^{-1}	391.241	0.872
	0.4	2.914	7.300×10^{-1}	1268.631	0.845
	1.0	3.235	7.407×10^{-1}	1657.559	0.842
	2.0	6.428	6.528×10^{-1}	5873.491	0.604

reaction kinetic equation provides a good fit for the iron-limiting condition (0.2-1.0 g-NZVI/L) but offers a poor description for the excess iron condition (2.0 g-NZVI/L). However, the rate constant correlates well with the NZVI dose under the iron-limiting condition (Fig. 3(b)). The Langmuir-Hinshelwood-type equation provides a good fit regardless of NZVI dose (Fig. 3(c)). The parameters of the Langmuir-Hinshelwood kinetic equation correlate well with the NZVI dose at 0.2 to 1.0 g-NZVI/L (Fig. 3(c)). It indicates that the reduction of nitrate to ammonia is clearly a heterogeneous catalytic reaction. In addition, when the NZVI dose is increased the reaction rate constant decreases and the adsorption constant increases, indicating that the nitrate adsorption is promoted by the abundance of NZVI (Fig. 3(c)). This behavior explains the significant T-N decrease at the beginning of the reaction for a high NZVI dose (Fig. 1(c)); that is, the fast nitrate adsorption leaves more unreacted nitrate on the NZVI surface. These results also support the hypothesis that adsorption is responsible for the apparent nitrate removal (Li *et al*., 2008).

3.2 Effects of Ionic Strength

Nitrate removal and ammonia generation were notably inhibited as the ionic strength increased (Fig. 4(a), (b)). The pseudo-second-order adsorption equation and the Langmuir-Hinshelwood kinetic formulation both gave good descriptions of nitrate and ammonia. Furthermore, the parameters correlate well with the NaCl concentration (Fig. 4(c), (d)). The description of the experimental results with the pseudo-first-order kinetic equation was poor for the nitrate but good for the ammonia because of the iron-limiting condition (Tables 3 and 4).

At a high electrolyte concentration, the enhanced electron transfer encourages Fe^0 corrosion, especially in the presence of Cl^- (Ma, 2012). It increases the available active sites and accelerates nitrate reduction (Ruangchainikom *et al*., 2006). However, a reaction can be inhibited by either the preferential sorption or the accumulation of Cl^- over nitrate in the Helmholtz layer. Chaplin *et al*. (2006) reported the acceleration of nitrate reduction by Pd-Cu/γ-Al_2O_3 at 50 mg/L Cl and the complete inhibition of nitrate reduction at 1000 mg/L Cl. In addition, the accelerated Fe^0 corrosion at high ionic strength enhances the production of OH^- (Gillham *et al.*, 2010; Ahn *et al.*, 2012). However, the pH increase was slightly faster at low NaCl concentration, in this study. The pH was 9.85, 9.59, and 9.36 at 5 min and 10.55, 10.30, and 10.12 at 45 min at 0.05, 0.1, and 0.5 M NaCl, respectively. The pH was stabilized at 10.51±0.05 (10.42-10.58) during 90-180 min, regardless of NaCl concentration. It indicates that the OH^- generated via Fe^0 corrosion was consumed to form iron (hydr)oxide precipitates and the amount of the precipitates are higher at high NaCl concentration because more OH^- is generated at high NaCl concentration. Considering the

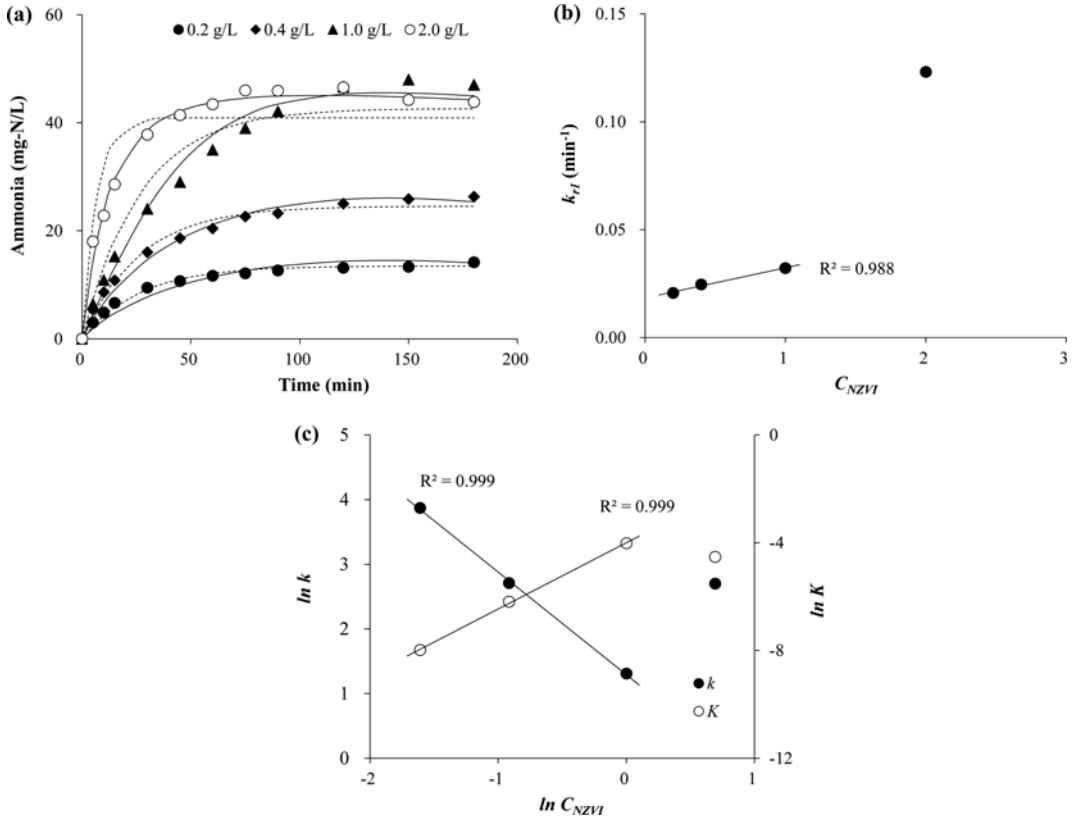

Fig. 3. (a) Ammonia Concentrations Predicted by Pseudo-first-order Reaction Kinetics (Dotted Lines) and by Langmuir-Hinshelwood Kinetics (Continuous Lines) for Different NZVI Doses (C_{NZVI}); the Correlation between the NZVI Dose (C_{NZVI}) and Kinetic Parameters for, (b) the Pseudo-first-order Rate Constant and for, (c) Langmuir-Hinshelwood Kinetics

Table 2. Kinetic Parameters of Ammonia Generation by NZVI for Different NZVI Doses

Kinetic model	NZVI (g/L)	Parameters		*SSE*	r^2
		k_{r1} (min^{-1})			
Pseudo first order reaction	0.2	2.06×10^{-2}		13.717	0.923
	0.4	2.463×10^{-2}		31.162	0.994
	1.0	3.216×10^{-2}		161.805	0.983
	2.0	1.231×10^{-1}		335.388	0.989
		k (L/mg-NH_3-N·min)	K (L/mg-NH_3-N)		
Langmuir-Hinshelwood kinetics	0.2	47.909	3.395×10^{-4}	18.265	0.997
	0.4	14.999	2.047×10^{-4}	10.545	0.990
	1.0	3.698	1.789×10^{-2}	56.443	0.979
	2.0	14.875	3.014×10^{-2}	26.488	0.965

results in this study that both nitrate removal and ammonia generation were inhibited at high NaCl concentration, it is regarded that the inhibition of nitrate adsorption by Cl^- adsorption and by iron (hydr)oxide precipitation affect more significantly to nitrate adsorption and reduction, than the promotion of electron transfer.

These phenomena are described well with the adsorption kinetic model in this study, which showed the increased adsorption rate and the decreased adsorption capacity for a high NaCl concentration (Fig. 4(b); Table 3). The high level of fitness of the Elovich equation (Table 3) at 0.05-0.5 M NaCl also suggests that an extent of NZVI surface is occupied by Cl^- and/or iron (hydr)oxides because the equations, in the form of the Elovich equation, consider the variation of chemisorption energetics in relation to the extent of surface coverage and the decrease in the sorption rate (Aharoni and Tompkins, 1970).

Meanwhile, adsorbate ions, which form relatively strong bonds with an adsorbent, are insensitive to ionic strength changes, whereas the adsorption of the adsorbates, which are weakly bound to an adsorbent, is significantly affected by ionic strength (Hayes *et al*., 1988). The effects of ionic strength also decrease when the surface coverage is not significant. Therefore, the significant suppression of nitrate adsorption at a high NaCl concentration indicates that relatively weak interactions, i.e., electrostatic attraction or hydrogen bonding, are predominant for nitrate adsorption on NZVI.

In addition, the surface charge of NZVI increased as ionic

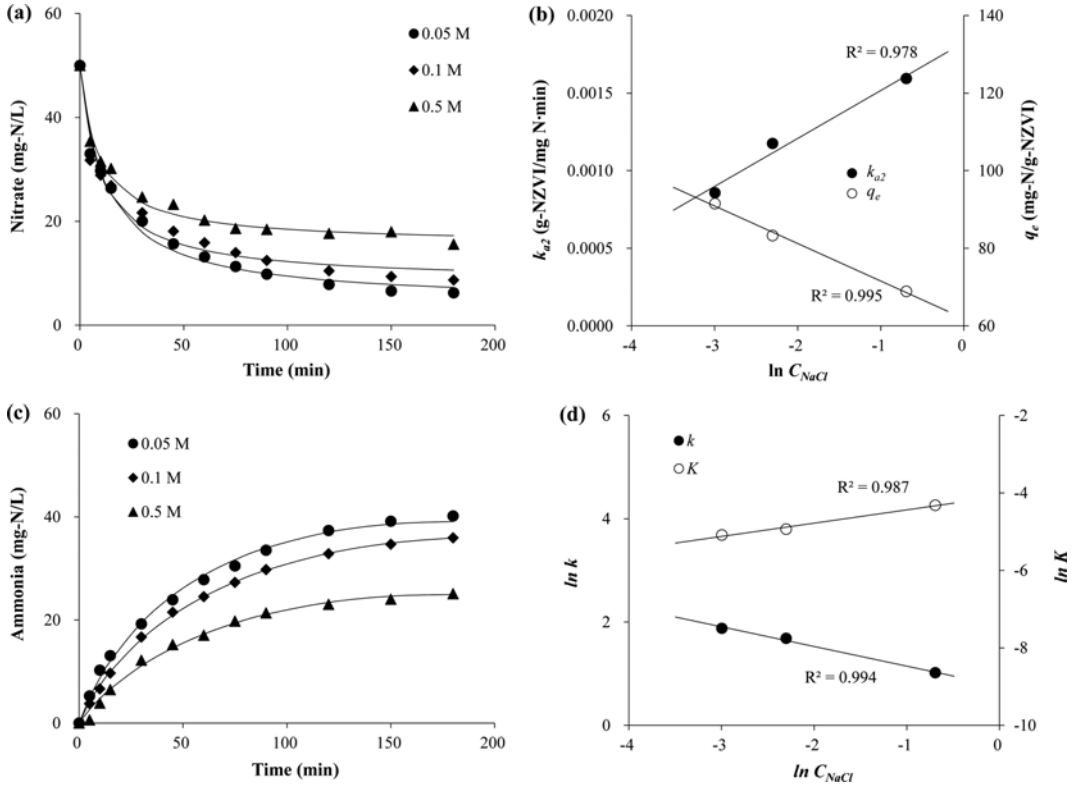

Fig. 4. (a) The Observed Nitrate Concentration and Prediction by Pseudo-second-order Adsorption Kinetics and, (b) the Correlation between the Parameters and the NaCl Concentration (C_{NaCl}), (c) the Observed Ammonia Concentration and Prediction by Langmuir-Hinshelwood Kinetics and, (d) the Correlation between the Parameters and C_{NaCl}

Table 3. Kinetic Parameters of Nitrate Removal by NZVI for Different NaCl Concentrations

Kinetic model	NaCl (M)	Parameters		*SSE*	r^2
		k_{r1} (min^{-1})			
Pseudo first order reaction	0.05	2.771×10^{-2}		403.18	0.794
	0.1	2.244×10^{-2}		617.991	0.615
	0.5	1.299×10^{-2}		811.838	0.263
		k_{a2} (g-NZVI/mg-N·min)	q_e (mg-N/g-NZVI)		
Pseudo second order adsorption	0.05	8.565×10^{-4}	91.495	28.5	0.985
	0.1	1.175×10^{-3}	83.251	45.264	0.972
	0.5	1.593×10^{-3}	68.838	16.587	0.985
		α (mg-N/g-NZVI·min)	β (g-NZVI/mg-N)		
Elovich equation	0.05	19.395	5.887×10^{-2}	7.864	0.996
	0.1	27.60	6.99×10^{-2}	5.113	0.997
	0.5	29.021	8.807×10^{-2}	8.853	0.992

strength increases. The proton sorption is known to be enhanced at high ionic strength (Saleh *et al.*, 2008). In this study, the pH was over the point of zero charge of 7.3-7.7 (Lin *et al.*, 2008; Satapanajaru *et al.*, 2011) after 5 min, regardless of reaction conditions. Therefore, the negative charge of NZVI surface could be more neutralized at high NaCl concentration. It was partially proved, in this study, by the promoted aggregation of NZVI particles as NaCl concentration increased. The size distribution of NZVI after a 5 min of reaction was analyzed with a particle size analyzer (PAMAS-2120, PAMAS). The mean size of the NZVI aggregates (χ_{50}, μm) and the NaCl concentration (C_{NaCl}, M) formed the following linear relationship:

$$\chi_{50} = 61.53 C_{NaCl} + 7.94 \quad (r^2 = 0.992) \tag{12}$$

The increased aggregate size indicates charge neutralization and subsequent decrease in NZVI stability and available surface area. Therefore, it seems reasonable that the overall charge of the system of NZVI, nitrate, nitrite, and ammonium is neutralized by the high electrolyte concentration.

3.3 Effects of the Initial pH

Confirming the observations of Wang *et al*. (2006) and Li *et al*.

Table 4. Kinetic Parameters of Ammonia Generation by NZVI for Different NaCl Concentrations

Kinetic model	NaCl (M)	Parameters		*SSE*	r^2
		k_{r1} (min^{-1})			
Pseudo first order reaction	0.05	3.165×10^{-2}		23.65	0.994
	0.1	3.009×10^{-2}		26.625	0.992
	0.5	2.663×10^{-2}		20.158	0.993
		k (L/mg-NH_3-N·min)	K (L/mg-NH_3-N)		
Langmuir-Hinshelwood kinetics	0.05	6.551	6.189×10^{-3}	8.207	0.996
	0.1	5.378	7.17×10^{-3}	1.154	0.999
	0.5	2.766	1.334×10^{-3}	7.162	0.992

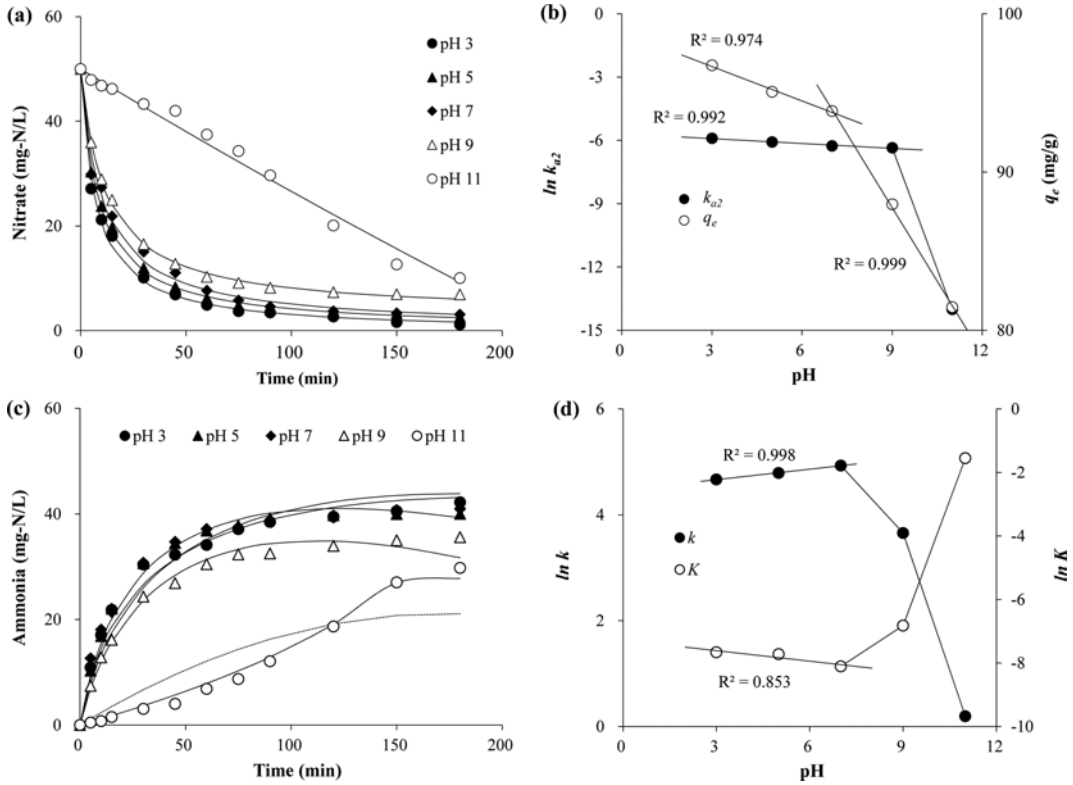

Fig. 5. (a) Observed Nitrate Concentration and Prediction by pseudo-second-order Adsorption Kinetics and, (b) the Correlation between the Parameters and the pH Value, (c) Observed Ammonia Concentration and Predictions by Langmuir-Hinshelwood Kinetics and, (d) the Correlation between the Parameters and the pH Value (The Dotted Line in, (c) Indicates the Prediction by Pseudo-first-order Reaction Kinetics for an Initial pH Value of 11)

Table 5. Kinetic Parameters of Nitrate Removal by NZVI for Different Initial pH Values

Kinetic model	pH	Parameters		SSE	r^2
		k_{r1} (min^{-1})			
Pseudo first order reaction	3	7.492×10^{-2}		165.52	0.929
	5	6.035×10^{-2}		182.453	0.922
	7	4.727×10^{-2}		239.178	0.896
	9	3.469×10^{-2}		322.932	0.849
	11	6.704×10^{-3}		130.775	0.939
		k_{a2} (g-NZVI/mg-N·min)	q_e (mg-N/g-NZVI)		
Pseudo second order adsorption	3	2.743×10^{-3}	$9.674\times10^{+1}$	10.838	0.995
	5	2.29×10^{-3}	$9.507\times10^{+1}$	5.064	0.998
	7	1.902×10^{-3}	$9.385\times10^{+1}$	27.627	0.988
	9	1.755×10^{-3}	$8.797\times10^{+1}$	2.803	0.999
	11	8.239×10^{-7}	$8.146\times10^{+1}$	30.7	0.986

Table 6. Kinetic Parameters of Ammonia Generation by NZVI for Different Initial pH Values

Kinetic model	pH	Parameters		*SSE*	r^2
		k_{r1} (min^{-1})			
Pseudo first order reaction	3	4.69×10^{-2}		71.715	0.964
	5	4.718×10^{-2}		55.997	0.972
	7	4.217×10^{-2}		125.827	0.935
	9	3.864×10^{-2}		13.763	0.991
	11	6.104×10^{-3}		242.656	0.797
		k (L/mg-NH_3-N·min)	K (L/mg-NH_3-N)		
Langmuir-Hinshelwood kinetics	3	106.366	4.705×10^{-4}	44.947	0.977
	5	120.082	4.42×10^{-4}	15.276	0.992
	7	138.391	3.02×10^{-4}	125.425	0.935
	9	38.658	1.09×10^{-3}	26.655	0.983
	11	1.216	2.121×10^{-1}	11.738	0.990

(2008), Fig. 5 shows a slight improvement in the nitrate removal and ammonia generation when pH decreased from 7 to 3. However, a notable inhibition was observed at a pH value of 9 and 11, and the profiles of nitrate and ammonia for a pH of 11 obviously differ from those of a pH range of 3 to 9. The pseudo-second-order adsorption kinetic equation provided good descriptions of the nitrate removal, and the parameters correlate well with the initial pH (Fig. 5(a), (b); Table 5). For the ammonia generation, the results of the Langmuir-Hinshelwood kinetic model and the pseudo-first-order reaction model are a good fit because of the iron-limiting condition. However, with more significant inhibition for a very high initial pH (11), only the Langmuir-Hinshelwood kinetic equation provided a good description of ammonia concentration (Fig. 5(c), (d) and Table 6). Clearly, the Langmuir-Hinshelwood kinetic model is more generally applicable.

Figure 5 illustrates that nitrate adsorption and ammonia generation are strongly inhibited at an initial pH of 9-11 and the kinetic parameters did not correlate well with initial pH, even though the concentrations of nitrate and ammonia were described well. It indicates a significant change in NZVI property. Note also that the profile of nitrate for a pH 11 can be divided into two stages which correspond to the reaction time of 0-15 min and 75-180 min (Fig. 5(a)). They correspond to before and after the reaction time when the pH level is stabilized at around 11. The initial pH of 11 decreased to 10.84 in the first 15 min, probably due to the consumption of OH^- (Lin *et al*., 2008a) and then increased gradually to 11.20±0.06 in the time frame of 75-180 min. It implies that the NZVI surface has been significantly changed by the accumulation of OH^- on NZVI and the formation of iron (hydr)oxide precipitates, e.g., $Fe(OH)_2$ (Gillham *et al.*, 2010). The nitrate is also in competition with the buffer compounds and other anions, such as HEPES (Yang and Lee, 2005; Hwang *et al*., 2010), phosphate buffer, and sodium sulfate (Zawaideh *et al*., 1998). Meanwhile, a sudden decrease in the nitrate removal rate, which was observed at initial pH of 9 in this study, has been reported by others for a pH of 9 with NZVI (Li *et al*., 2008) for a pH of 6.7 with NZVI immobilized on graphite (Huan *et al*., 2006), and for a pH of 5 with an Ni-Cu/TiO_2 catalyst (Gao *et al*., 2004).

NZVI reactivity can be enhanced at a low pH level by washing the passivation film of iron (hydr)oxide on the NZVI surface, to increase the availability of electrons from Fe^0 core (Huan *et al*., 2006; Wang *et al*., 2009). The removal of passivation film enhances the reaction between iron and water (Eq. (13)) to enhance hydrogen gas production (Liu *et al.*, 2005). The abundance of H^+ can also lead to the acceleration of hydrogenation of nitrate (Pintar *et al.*, 1996).

$$Fe^0 + 2H_2O \rightarrow Fe^{2+} + H_2(\uparrow) + 2OH^- \quad (13)$$

However, In this study, the pH effect was not significant for the initial pH of 3-7, because there was a rapid rise of the pH, as a result of OH^- production via the anaerobic corrosion of Fe^0 (Lin *et al*., 2008b). The pH level remained at 10.13 ± 0.11 after 15 min, regardless of the initial pH. The pH increase has also been reported in studies with microscale iron particles. Huang *et al*. (1998) observed that the pH was increased to 4, 4.5, and 7 when the initial pH was 2, 3, and 4, respectively, during nitrate reduction with 6-10 μm iron particles. They reported that all the nitrate was removed before the rise in the pH, and the enhancement of nitrate reduction at low pH was not significant.

4. Conclusions

In this study, adsorption kinetic equations and heterogeneous catalytic reaction kinetic equations were proposed and tested for nitrate reduction by NZVI. The kinetic models with the best fit were used to investigate the effect of the initial pH and ionic strength. The results have led to the following conclusions:

1. The widely used pseudo first order reaction model provides a poor fit for both the nitrate removal by NZVI in an iron-limiting condition and the ammonia generation in an excess iron condition. However, the reaction rate constant correlates well with the NZVI dose, the initial pH, and the ionic strength.
2. Regardless of the reaction conditions of this study, the pseudo-first-order and pseudo-second-order adsorption kinetic equations provided a good fit for the nitrate removal whereas the Langmuir-Hinshelwood kinetic equation provided a good fit for the ammonia generation. In addition, the kinetic parameters correlate well with the reaction conditions, unless the reactivity or property of NZVI was greatly changed by a

very high NZVI dose or by the enhanced iron (hydr)oxides formation at a very high initial pH. This correlation strongly indicates that the apparent nitrate removal is by adsorption, that the nitrate reduction by NZVI is a heterogeneous catalytic reaction, and that the kinetic models have great potential for describing and predicting nitrate reduction by NZVI under a variety of reaction conditions. These models all help to explain the initial T-N decrease during NZVI-induced nitrate reduction, a phenomenon observed in this study and in many other studies. In addition, the Elovich equation offers a good description of the inhibition caused by an increase in NaCl.

3. The nitrate adsorption and ammonia generation are both faster with a high NZVI dose, a low ionic strength, and a low initial pH. However, the inhibition that occurs with a high initial pH is more significant than the promotion at a low initial pH. The adsorption rate constant is highly dependent on NaCl concentration and on pH, in the range of 7-11, indicating that the electrostatic attraction or hydrogen bonding is predominant for nitrate adsorption on NZVI. In addition, the NZVI aggregation promoted at a high NaCl concentration and the competition of nitrate with hydroxyl anions was observed at a high initial pH.

Acknowledgements

This research was supported by Basic Science Research Program through the National Research Foundation of Korea (NRF) funded by the Ministry of Education (2013R1A1A2059853).

References

Aharoni, C. and Tompkins, F. C. (1970). "Kinetics of adsorption and desorption and the elovich equation." *Advanced Catalysis*, Vol. 21, pp. 1-49, DOI: 10.1016/S0360-0564(08)60563-5.

Ahn, H., Jo, H. Y., Kim, G.-Y., and Koh, Y.-K. (2012). "Effect of NaCl on Cr(VI) Reduction by Granular Zero Valent Iron (ZVI) in Aqueous Solutions." *Mater. Trans.*, Vol. 53, No. 7, pp. 1324-1329, DOI: 10.2320/matertrans.M2011375.

Alidokht, L., Khataeea, A. R., Reyhanitabar, A., and Oustan, S. (2011). "Reductive removal of Cr(VI) by starch-stabilized Fe^0 nanoparticles in aqueous solution." *Desalination*, Vol. 270, Nos. 1-3, pp. 105-110. DOI: 10.1016/j.desal.2010.11.028.

Alowitz, M. J. and Scherer, M. M. (2002). "Kinetics of nitrate, nitrite, and Cr(VI) reduction by iron metal." *Environ. Sci. Technol.*, Vol. 36, pp. 299-306, DOI: 10.1021/es011000h.

Andreas, T., Silke, T., Yuri, K., and Aharon, G. (2009). "Chloroethene dehalogenation with ultrasonically produced air-stable nano iron." *Ultrason. Sonochem.*, Vol. 16, pp. 617-621, DOI: 10.1016/j.ultsonch.2009.01.005.

APHA, AWWA and WEF (1998). *Standard methods for the examination of water and wastewater,* American Public Health Association, American Water Works Association, Water Environment Federation. Washington, DC, W.A.

Cáceres-Jensen, L., Rodríguez-Becerra, J., Parra-Rivero, J., Escudey, M., Barrientosa, L., and Castro-Castillo, V. (2013). "Sorption kinetics of diuron on volcanic ash derived soils." *J. Hazard. Mater.*, Vol. 261, pp. 602-613, DOI: 10.1016/j.jhazmat.2013.07.073.

Chaplin, B. P., Roundy, E., Guy, K. A., Shapley, J. R., and Werth, C. J. (2006). "Effects of natural water ions and humic acid on catalytic nitrate reduction kinetics using an alumina supported Pd-Cu catalyst." *Envir. Sci. Technol.*, Vol. 40, pp. 3075-3081. DOI: 10.1021/es0525298.

Cheung, W. H., Szeto, Y. S., and McKay, G. (2007). "Intraparticle diffusion processes during acid dye adsorption onto chitosan." *Bioresource Technol.*, Vol. 98, pp. 2897-2904, DOI: 10.1016/j.biortech.2006.09.045.

Choe, S., Chang, Y. Y., Hwang, K. Y., and Khim, J. (2000). "Kinetics of reductive denitrification by nanoscale zero-valent iron." *Chemosphere*, Vol. 41, No. 8, pp. 1307-1311, DOI: 10.1016/S0045-6535(99)00506-8.

Gao, W., Jin, R., Chen, J., Guan, X., Zeng, H., Zhang, F., and Guan N. (2004). "Titania-supported bimetallic catalysts for photocatalytic reduction of nitrate." *Catal. Today*, Vol. 90, Nos. 3-4, pp. 331-336, DOI: 10.1016/j.cattod.2004.04.043.

García-Figueruelo, C., Bes-Piá, A., Mendoza-Roca, J. A., Lora-García, J., and Cuartas-Uribe, B. (2009). "Reverse osmosis of the retentate from the nanofiltration of secondary effluents." *Desalination*, Vol. 240, pp. 274-279, DOI: 10.1016/j.desal.2008.01.052.

Gillham, R. W., Vogan, J., Gui, L., Duchene, M., and Son, J. (2010). *Iron barrier walls for chlorinated solvent remediation,* In: Stroo HF, Ward CH, editors, *In Situ Remediation of Chlorinated Solvent Plumes*, Springer, New York.

Hameed, B. H., Tan, I. A. W., and Ahmad, A. L. (2008). "Adsorption isotherm, kinetic modeling and mechanism of 2,4,6-trichlorophenol on coconut husk-based activated carbon." *Chem. Eng. J.*, Vol. 144, No. 2, pp. 235-244, DOI: 10.1016/j.cej.2008.01.028.

Hayes, K. F., Papelis, C., and Leckie, J. O. (1988). "Modeling ionic strength effects on anion adsorption at hydrous oxide/solution interfaces." *J. Colloid Interf. Sci.*, Vol. 125, No. 2, pp. 717-726, DOI: 10.1016/0021-9797(88)90039-2.

Ho, Y. S. and Ofomaja, A. E. (2006). "Pseudo-second-order model for lead ion sorption from aqueous solutions onto palm kernel fiber." *J. Hazard. Mater.*, Vol. 129, Nos. 1-3, pp. 137-142, DOI: 10.1016/j.jhazmat.2005.08.020.

Huan, A., Zhao-hui, J., Lu, H., and Cheng-hua, Q. (2006). "Synthesis of nanoscale zero-valent iron supported on exfoliated graphite for removal of nitrate." *T. Nonferr. Metal. Soc.*, Vol. 16, pp. 345-349, DOI: 10.1016/S1003-6326(06)60207-0.

Huang, C.-P., Wang, H.-W., and Chiu, P.-C. (1998). "Nitrate reduction by metallic iron." *Water Res.*, Vol. 32, No. 8, pp. 2257-2264, DOI: 10.1016/S0043-1354(97)00464-8.

Huang, Y. H., Zhang, T. C., Shea, P. J., and Comfort, S. D. (2003), "Effects of oxide coating and selected cations on nitrate reduction by iron metal." *J. Environ. Qual.*, Vol. 32, pp. 1306-1315, DOI: 10.2134/jeq2003.1306.

Huang, Y. H. and Zhang, T. C. (2004). "Effects of low pH on nitrate reduction by iron powder." *Water Res.*, Vol. 38, pp. 2631-2642, DOI: 10.1016/j.watres.2004.03.015.

Hwang, Y., Kim, D., Ahn, Y.-T., Moon, C.-M., and Shin, H.-S. (2012). "Recovery of ammonium salt from nitrate-containing water by iron nanoparticles and membrane contactor." *Environ. Eng. Res.*, Vol. 17, No. 2, pp. 111-116, DOI: /10.4491/eer.2012.17.2.111.

Hwang, Y. H., Kim, D. G., Ahn, Y. T., Moon, C. M., and Shin, H.S. (2010). "Fate of nitrogen species in nitrate reduction by nanoscale zero valent iron and characterization of the reaction kinetics." *Water Sci. Technol.*, Vol. 61, No. 3, pp. 705-712, DOI: 10.2166/wst.2010.895.

Li, T., Zhang, Y., Geng, B., Wang, D., Wang, S., and Jin, Z. (2008).

"Preparation of nanoiron by water-in-oil (W/O) microemulsion for reduction of nitrate in water." *Proc. 2nd Int. Conf. on Bioinformatics and Biomedical Engineering, Shanghai, China,* ICBBE 2008, pp. 3339-3342. DOI: 10.1109/ICBBE.2008.1164.

Lin, K.-S., Chang, N.-B., and Chuang, T.-D. (2008a). "Fine structure characterization of zero-valent iron nanoparticles for decontamination of nitrites and nitrates in wastewater and groundwater." *Sci. Technol. Adv. Mater.*, Vol. 9, 025015 (9 pp), DOI: 10.1088/1468-6996/9/2/025015.

Lin, Y.-T., Weng, C.-H., and Chen, F.-Y. (2008b). "Effective removal of AB24 dye by nano/micro-size zero-valent iron." *Sep. Purif. Technol.*, Vol. 64, pp. 26-30, DOI: 10.1016/j.seppur.2008.08.012.

Liou, T. H., Lo, S.-L., Lin, C.-J., Hui, W. K., and Weng, S. C. (2005). "Chemical reduction of an unbuffered nitrate solution using catalyzed and uncatalyzed nanoscale iron particles." *J. Hazard. Mater.*, Vol. 127, Nos. 1-3, pp. 102-110, DOI: 10.1016/j.jhazmat.2005.06.029.

Liu, H. B., Chen, T. H., Chang, D. Y., Chen, D., Liu, Y., He, H. P., and Yuan, R. F. (2012). "Nitrate reduction over nanoscale zero-valent iron prepared by hydrogen reduction of goethite." *Mater. Chem. Phys.*, Vol. 133, No. 1, pp. 205-211, DOI: 10.1016/j.matchemphys.2012.01.008.

Liu, Y., Majetich, S. A., Tilton, R. D., Sholl, D. S., and Lowry, G. V. (2005). "TCE dechlorination rates, pathways, and efficiency of nanoscale iron particles with different properties." *Environ. Sci. Technol.*, Vol. 39, pp. 1338-1345, DOI: 10.1021/es049195r.

Luo, J., Song, G., Liu, J., Qiana, G., and Xu, Z. P. (2014). "Mechanism of enhanced nitrate reduction via micro-electrolysis at the powdered zero-valent iron/activated carbon interface." *J. Colloid Interf. Sci.*, Vol. 435, No. 1, pp. 21-25, DOI: 10.1016/j.jcis.2014.08.043.

Ma, F.-Y. (2012). *Corrosive effects of chlorides on metals*, Pitting Corrosion, Prof. Nasr Bensalah (Ed.), InTech, Rijeka, Croatia.

Özacar, M. and Şengil, I. A. (2005). "A kinetic study of metal complex dye sorption onto pine sawdust." *Process Biochem.*, Vol. 40, No. 2, pp. 565-572, DOI: 10.1016/j.procbio.2004.01.032.

Öztürk, N. and Bektaş, T. E. (2004). "Nitrate removal from aqueous solution by adsorption onto various materials." *J. Hazard. Mater.*, Vol. B112, pp. 155-162, DOI: 10.1016/j.jhazmat.2004.05.001.

Patoczka, J. and Wilson, D. J. (1984). "Kinetics of the desorption of ammonia from water by diffused aeration." *Separ. Sci. Technol.*, Vol. 19, No. 1, pp. 77-93, DOI:10.1080/01496398408059939.

Petala, E., Dimos, K., Douvalis, A., Bakas, T., Tucek, J., Zboøil, R., and Karakassides, M. A. (2013). "Nanoscale zero-valent iron supported on mesoporous silica: Characterization and reactivity for Cr(VI) removal from aqueous solution." *J. Hazard. Mater.*, Vol. 261, pp. 295-306, DOI: 10.1016/j.jhazmat.2013.07.046.

Pintar, A., Batista, J., Levee, J., and Kajiuchi, T. (1996). "Kinetics of the catalytic liquid-phase hydrogenation of aqueous nitrate solutions." *Appl. Catal. B-Enviro.*, Vol. 11, pp. 81-98, DOI: 10.1016/S0926-3373(96)00036-7.

Quan, X., Wang, F., Zhao, Q., Zhao, T., and Xiang, J. (2009). "Air stripping of ammonia in a water-sparged aerocyclone reactor." *J. Hazard. Mater.*, Vol. 170, pp. 983-988, DOI: 10.1016/j.jhazmat.2009.05.083.

Ruangchainikom, C., Liao, C.-H., Anotai, J., and Lee, M.-T. (2006). "Effects of water characteristics on nitrate reduction by the Fe^0/CO_2 process." *Chemosphere*, Vol. 63, No. 2, pp. 335-343, DOI: 10.1016/j.chemosphere.2005.06.049.

Saleh, N., Kim, H. J., Phenrat, T., Matyjaszewski, K., Tilton, R. D., and Lowry, G. V. (2008). "Ionic strength and composition affect the mobility of surface-modified Fe^0 nanoparticles in water-saturated sand columns." *Envir. Sci. Technol.*, Vol. 42, No. 9, pp. 3349-55, DOI: 10.1021/es071936b.

Satapanajaru, T., Chompuchan, C., Suntornchot, P., and Pengthamkeerati, P. (2011). "Enhancing decolorization of Reactive Black 5 and Reactive Red 198 during nano zerovalent iron treatment." *Desalination*, Vol. 266, pp. 218-230, DOI: 10.1016/j.desal.2010.08.030.

Spiro, M. (1989). *Chemical kinetics*, in: R.G. Compton (Ed.), Reactions the Liquid–Solid Interface, Vol. 28, Elsevier, Amsterdam.

Su, C. and Puls, R. W. (2004). "Nitrate reduction by zerovalent iron: effects of formate, oxalate, citrate, chloride, sulfate, borate, and phosphate." *Envir. Sci. Technol.*, Vol. 38, No. 9, pp. 2715-2720, DOI: 10.1021/es034650p.

Wang, C. B. and Zhang, W. X. (1997). "Synthesizing nanoscale iron particles for rapid and complete dechlorination of TCE and PCBs." *Envir. Sci. Technol.*, Vol. 31, pp. 2154-2156, DOI: 10.1021/es970039c.

Wang, Q., Snyder, S., Kim, J., and Choi, H. (2009). "Aqueous ethanol modified nanoscale zerovalent iron in bromate reduction: Synthesis, characterization, and reactivity." *Envir. Sci. Technol.*, Vol. 43, pp. 3292-3299, DOI: 10.1021/es803540b.

Wang, W., Jin, Z., Li, T., Zhang, H., and Gao S. (2006). "Preparation of spherical iron nanoclusters in ethanol–water solution for nitrate removal." *Chemosphere*, Vol. 65, pp. 1396-1404, DOI: 10.1016/j.chemosphere.2006.03.075.

Yang, G. C. C., and Lee, H.-L. (2005). "Chemical reduction of nitrate by nanosized iron: kinetics and pathways." *Water Res.*, Vol. 39, No. 5, pp. 884-894, DOI: 10.1016/j.watres.2004.11.030.

Zawaideh, L. L. and Zhang, T. C. (1998). "The effects of pH and addition of an organic buffer (HEPES) on nitrate transformation in Fe^0-water systems." *Water Sci. Technol.*, Vol. 38, No. 7, pp. 107-115, DOI: 10.1016/S0273-1223(98)00613-1.

Zhang, R., Li, J., Liu, C., Shen, J., and Sun, X. (2013). "Reduction of nitrobenzene using nanoscale zero-valent iron conned in channels of ordered mesoporous silica." *Colloid. Surface. A*, Vol. 425, pp. 108-114, DOI: 10.1016/j.colsurfa.2013.02.040.

Zhang, X., Lin, Y., and Chen, Z. (2009). "2,4,6-Trinitrotoluene reduction kinetics in aqueous solution using nanoscale zero-valent iron." *J. Hazard. Mater.*, Vol. 165, Nos. 1-3, pp. 923-927, DOI: 10.1016/j.seppur.2010.10.015.

Zhou, Y., Lu, P., and Lu, J. (2012). "Application of natural biosorbent and modified peat for bisphenol A removal from aqueous solutions." *Carbohyd. Polym.*, Vol. 88, No. 2, pp. 502-508, DOI: 10.1016/j.carbpol.2011.12.034.

Appendix.

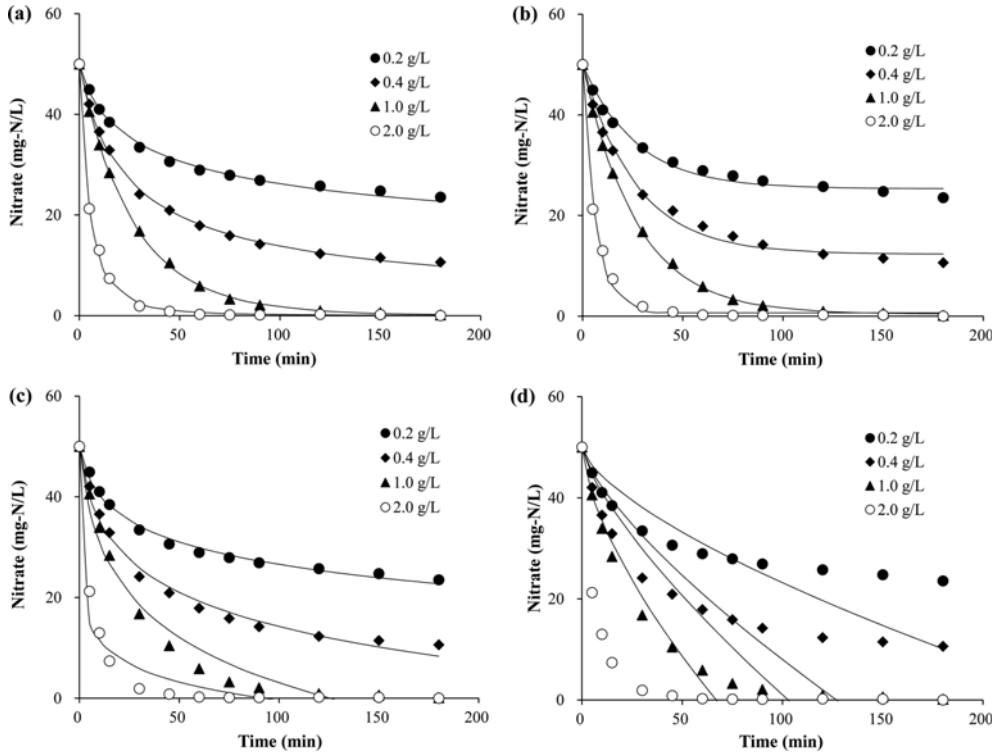

Fig. 6. Predictions of Nitrate Concentration from: (a) an Nth-order Model, (b) Pseudo-first-order Adsorption Kinetics, (c) the Elovich Equation, (d) an Intraparticle Diffusion model for Different NZVI Doses (*CNZVI*)

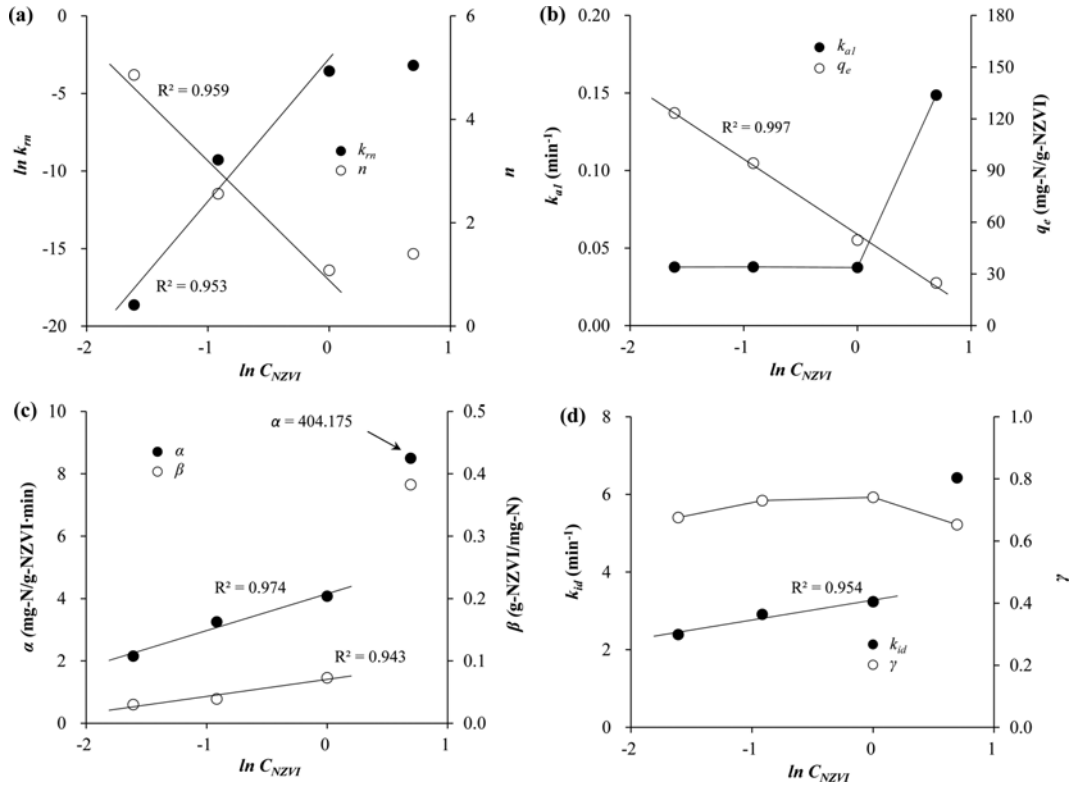

Fig. 7. Correlations between the NZVI dose (*CNZVI*) and Parameters of: (a) an Nth-order Model, (b) Pseudo-first-order Adsorption Kinetics, (c) the Elovich Equation, (d) an Intraparticle Diffusion Model